Adding connections can hinder network synchronization of time-delayed oscillators

Joseph D. Hart, Jan Philipp Pade, Tiago Pereira, Thomas E. Murphy, and Rajarshi Roy

Phys. Rev. E **92**, 022804 — Published 10 August 2015

DOI: 10.1103/PhysRevE.92.022804

Adding connections can hinder network synchronization of time-delayed oscillators

Joseph D. Hart,[1,2] Jan Philipp Pade,[3] Tiago Pereira,[4,5] Thomas E. Murphy,[1,6] and Rajarshi Roy[1,2,7]

[1] *Institute for Research in Electronics and Applied Physics, University of Maryland, College Park, MD 20742*

[2] *Department of Physics, University of Maryland, College Park, MD 20742*

[3] *Humboldt University of Berlin, Institude of Mathematics, Unter der Linden 6, 10099 Berlin, Germany*

[4] *Department of Mathematics, Imperial College London, London SW72AZ, UK*

[5] *Instituto de Ciências Matemáticas e de Computação, Universidade de São Paulo, 13560-970 São Carlos, São Paulo Brazil*

[6] *Department of Electrical and Computer Engineering, University of Maryland, College Park, MD 20742*

[7] *Institute for Physical Science and Technology, University of Maryland, College Park, MD 20742*

We provide the first experimental evidence that adding links to a network's structure can hinder synchronization. Our experiments and theoretical analysis of networks of time-delayed optoelectronic oscillators uncover the scenario of loss of identical synchronization upon connectivity modifications. This counterintuitive loss of synchronization can occur even when the network structure is improved from a connectivity perspective. Utilizing a master stability function approach, we show that a time delay in the coupling of nodes plays a crucial role in determining a network's synchronization properties, and that this effect is more prominent in directed networks than in undirected networks, especially for large networks. Our results provide insight into the impact of structural modifications in networks with equal coupling delays and open the path to design changes to the network connectivity to sustain and control the performance of real-world networks.

PACS numbers: 05.45.Xt, 89.75.-k

I. INTRODUCTION

Synchronization crucially affects the performance of many real-world complex networks. Synchrony between nodes is often desirable, such as in the transmission of information in sensor networks [1, 2]; however, it can also be pathological as in the case of epileptic seizures caused by synchronously firing neurons [3]. Hence, an important open question with practical consequences is how modifications of the network linking structure affect its ability to synchronize [4]. Recent work has revealed that enhancements to the network connectivity can lead to synchronization failure. Indeed, in networks with community structure, adding links to enhance the community can lead to a fragile synchronization [5, 6], and in power-grid models adding new lines can cause a break of synchrony [7–10]. Moreover, even structural improvements such as decreasing the network diameter by introducing new links can lead to synchronization loss [11]. Despite recent progress, the problem of determining the importance of individual links on dynamics has yet to be resolved.

This problem is further complicated when considering real networks, in which a time delay in the coupling is often present due to the finite propagation time of signals. Examples of such networks include gene-regulatory networks [12], neural networks [13], and power systems engineering [14]. While it has long been understood that the introduction of time delays can substantially affect the dynamical properties of a network [15], the ubiquity of time delay in physical networks and the complexity of the behaviors that often result have led to much recent interest in the synchronization of oscillator networks with time-delayed coupling [16–20]. As we will show in our real experimental networks, the presence of time delay in the coupling plays a fundamental role in determining the impact of adding a single link on a network's synchronization properties.

In this work we provide a first experimental demonstration of the counterintuitive phenomenon that adding a link to the network structure can hinder synchronization. Our experimental and theoretical analysis on optoelectronic oscillators with time-delayed coupling reveal the mechanism for synchronization loss: once extra connections are included, the spectrum of the network Laplacian can undergo changes leading to the appearance of instabilities in global synchronization. Such drastic changes can occur even when the network structure is improved. Additionally, by combining recent results on the master stability function approach and the spectral theory of networks, we demonstrate that a time delay in the coupling of nodes plays a crucial role in determining a network's synchronization properties, and that this effect is more prominent in directed networks than in undirected networks.

II. EXPERIMENTAL SETUP

For concreteness in experimental demonstrations, we consider three network configurations with four nodes each, shown in Fig. 1. The coupling links of the initial network are shown as solid black lines, and the added link is shown as a dashed gray (red online) line, with the arrows indicating the direction of the coupling.

The experiment consists of a network of four identical

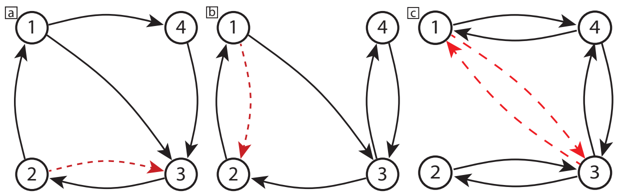

FIG. 1. (color online) Schematics of the directed four node networks considered. (a)Directed Network 1. (b) Directed Network 2. (c) Undirected Network. The addition of the dashed gray (red online) link causes a decrease in the stability of global synchronization. All links are weighted equally. The self-feedback and coupling delay time τ and roundtrip gain β are the same for each node.

optoelectronic, time-delayed feedback loops, which have been studied previously [21–24]. An extensive review of the dynamics and applications of such oscillators is given in Ref. [25]. Each node consists of a laser diode whose beam passes through a Mach-Zehnder modulator (MZM) before being converted to an electrical signal by a photodiode. This signal is one input to the digital signal processing board (DSP). The incoming coupling signals are optically combined and converted to an electrical signal by a second photodiode. This electrical signal serves as the second input to the DSP, which then implements the time delay, coupling, and digital filtering. The digital filter is a two-pole bandpass filter with cutoff frequencies $\omega_H/2\pi = 100$ Hz and $\omega_L/2\pi = 2.5$ kHz and sampling rate 24 kSamples/s. The DSP output is amplified to achieve a total feedback strength β, which effectively controls the complexity of the node dynamics. This amplified electrical signal is then used to drive the MZM. A schematic of the apparatus can be found in Ref. [22]. The equations governing the dynamics of the optoelectronic network are derived in Ref. [21] and are given by

$$\dot{\mathbf{u}}_i(t) = \mathbf{E}\mathbf{u}_i(t) - \mathbf{F}\beta\cos^2(x_i(t-\tau)+\phi_0), \quad (1)$$

$$x_i(t) = \mathbf{G}\Big(\mathbf{u}_i(t) - \epsilon\sum_j l_{ij}\mathbf{u}_j(t)\Big) \quad (2)$$

where

$$\mathbf{E} = \begin{bmatrix} -(\omega_L+\omega_H) & -\omega_L \\ \omega_H & 0 \end{bmatrix},\ \mathbf{F} = \begin{bmatrix} \omega_L \\ 0 \end{bmatrix},\ \text{and } \mathbf{G} = \begin{bmatrix} 1 & 0 \end{bmatrix}.$$

Here $\mathbf{u}_i$ is a $2{\times}1$ vector describing the state of the digital filter at node i, and $x_i(t)$ is the observed variable, the normalized voltage of the electrical input to the MZM. The nodes are diffusively coupled by the Laplacian coupling matrix $\mathbf{L} = (l_{ij})$; the diagonal element $l_{ii} \geq 0$ is the sum of the incoming coupling strengths to node i, and the off-diagonal element l_{ij} is the opposite of the coupling strength from node j to node i. Diffusive coupling ensures the existence of the globally synchronized state. Since we consider only identical coupling strengths, we have $l_{ii} = n_{in}$, the number of incoming links to node i. In this experiment, the time delay of the self-feedback and coupling are set to be $\tau = 1.5$ ms; however, simulation shows that the stability of global synchronization is independent of the delay times, as long as the self-feedback and coupling delays are equal. The effect of changing the coupling delay while keeping the self-feedback delay constant is not investigated here but has been studied previously [24]. We choose the phase bias $\phi_0 = \pi/4$ so that for small feedback strength, the MZM is operated in the linear regime. This ensures that for small β the system displays nearly sinusoidal periodic dynamics. At large β the MZM nonlinearity becomes important and the system behaves chaotically. The dynamics of an individual, uncoupled oscillator in each of these regimes is shown in the insets to Fig. 2. The global coupling strength ϵ is chosen such that global synchronization is stable for the initial network. The dynamics of an uncoupled node can be modeled by setting $\epsilon = 0$, since the second term in Eq. (2) represents the diffusive coupling scheme.

In order to distinguish synchronized states from desynchronized states, we define the global synchronization error

$$\theta(t) = \frac{1}{N(N-1)}\sum_{i,j}|x_i(t) - x_j(t)|, \quad (3)$$

where N is the total number of nodes. For globally synchronized states θ ideally approaches zero, while for desynchronized states θ is non-zero. In practice, due to experimental mismatch and noise, real networks that synchronize approach a synchronization floor that is small but non-zero.

III. DIRECTED NETWORKS

We first consider the general case of directed networks. We demonstrate the destabilization of global synchrony upon the addition of a new link with two different classes of node dynamics, periodic ($\beta = 1.35$) and chaotic ($\beta = 4.5$), shown in the insets of Fig. 2. Figure 2 shows the simulated global synchronization error for both the periodic and chaotic cases of the two network configurations. The nodes start from random initial conditions. The initial network coupling is turned on at $t = 40$ ms, and synchronous dynamics are observed. At $t = 120$ ms, the new link is added, destabilizing the synchronized state. Moreover, our results show that both synchronization and desynchronization are not transient. Thus, our simulations show that the globally synchronized state can be destabilized by the addition of a single link to the network.

We now test these predictions in a real experimental network of optoelectronic oscillators. For each trial of the experiment, the nodes are started from random initial conditions by recording the random electrical feedback at the input to the DSP board for 10 ms before enabling feedback. Feedback without coupling is then

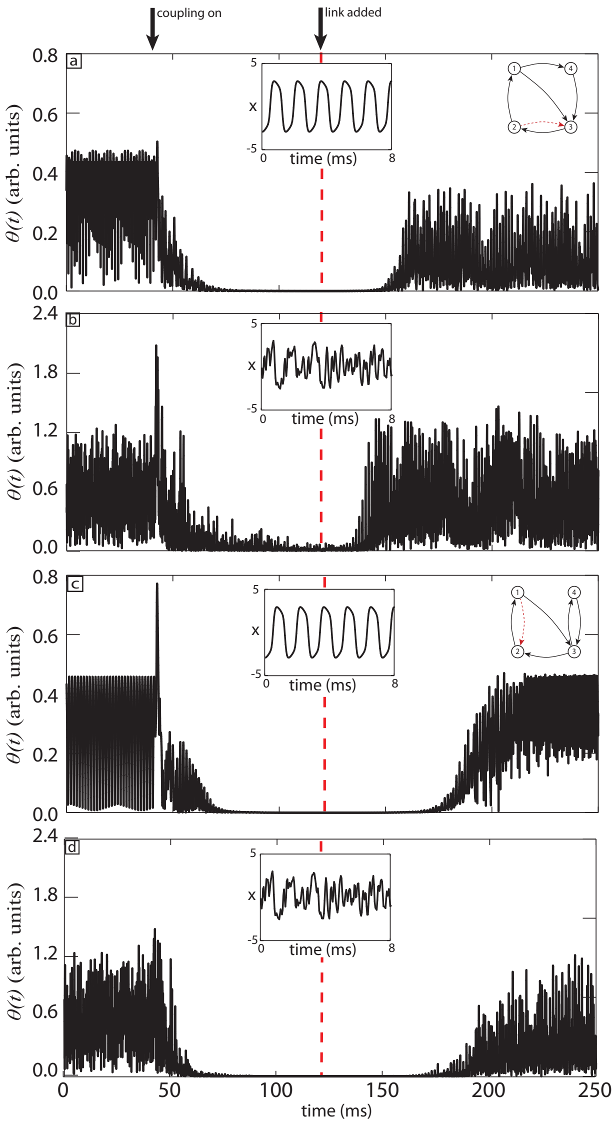

FIG. 2. (color online) Simulated loss of synchrony upon the addition of a link for the two networks shown. The new link is added at $t = 120$ ms, indicated by the dashed line. The synchronous dynamics are periodic ($\beta = 1.35$) for (a) and (c) and chaotic ($\beta = 4.5$) for (b) and (d). The ϵ values used for (a)-(d) are 0.85, 0.49, 0.90, and 0.53, respectively. Inset: Dynamics of a single uncoupled node.

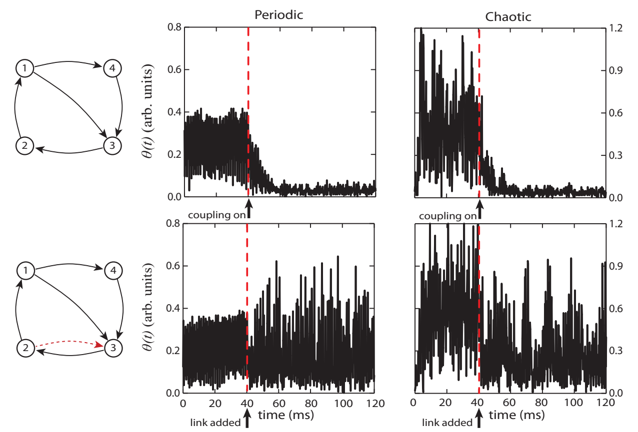

FIG. 3. (color online) Experimental results for Direct Network 1. In all cases, the nodes are initially uncoupled. The coupling scheme depicted to the left is implemented at t=40 ms as indicated by the dashed line. For the periodic case, $\epsilon = 0.85$ and for the chaotic case $\epsilon = 0.49$, which are the same values used in simulation.

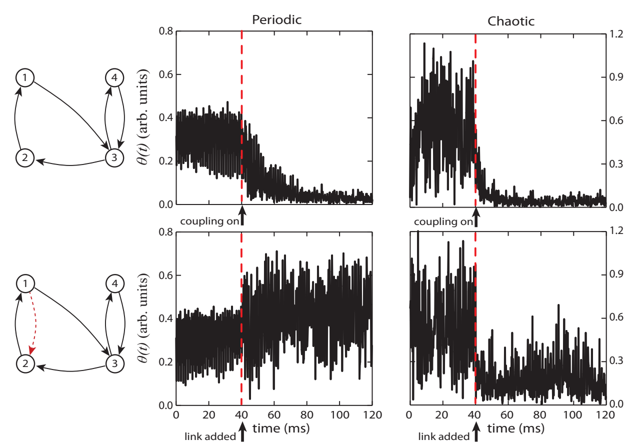

FIG. 4. (color online) Experimental results for Direct Network 2. In all cases, the nodes are initially uncoupled. The coupling scheme depicted to the left is implemented at t=40 ms as indicated by the dashed line. For the periodic case, $\epsilon = 0.90$ and for the chaotic case $\epsilon = 0.53$, which are the same values used in simulation.

enabled for 90 ms in order for transients to die out. At the end of this period, coupling is turned on. Since the network structure of our apparatus cannot be changed during an experiment, we first test the stability of global synchrony on the initial network. Then starting from different random initial conditions, we test the stability with the new link added. Figures 3 and 4 show experimental measurements for the periodic and chaotic cases on Network 1 and Network 2, respectively. We find in all cases that the experiment and simulation agree: global synchronization is stable in the initial networks and unstable in the networks with the added link.

To investigate the transition from stability to instability of the globally synchronized state we use the master stability function (MSF) approach [26, 27] and its extension to time-delayed systems [19, 20]. Linearizing Eqs. (1) and (2) about the globally synchronous state, we obtain the variational equation

$$\begin{aligned}\delta\dot{\mathbf{u}}(t) = \mathbf{E}\delta\mathbf{u}(t) + \mathbf{F}\beta\sin(2x_s(t-\tau) + 2\phi_0) \\ \times\, \mathbf{G}(1-\epsilon\gamma_k)\delta\mathbf{u}(t-\tau),\end{aligned} \tag{4}$$

where the γ_k are the eigenvalues of the Laplacian coupling matrix $\mathbf{L}$ and x_s stands for the synchronized solution (either periodic or chaotic). The zero eigenvalue corresponds to perturbations parallel to the synchronization

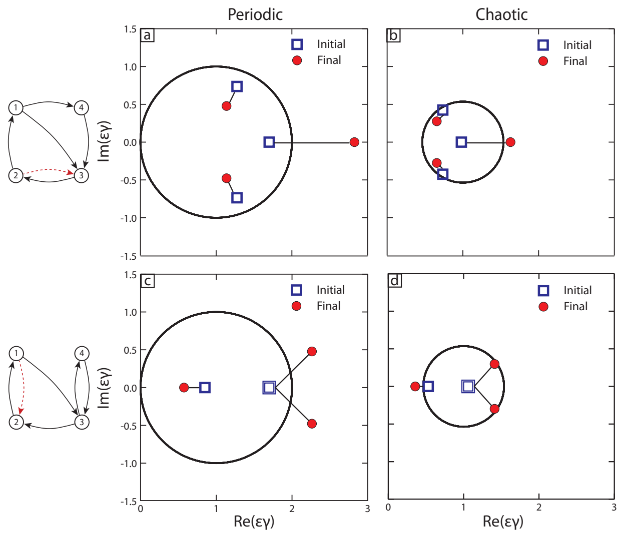

FIG. 5. (color online). Transition of global synchrony from stable to unstable upon the addition of a link. (a),(b) MSF and Laplacian eigenvalue spectra for Network 1. (c),(d) MSF and Laplacian eigenvalue spectra for Network 2. The eigenvalues of the original network are represented by □, and those of the network with the link added are represented by ●. The thick line denotes the zero contour of the MSF: inside global synchrony is stable; outside it is unstable.

manifold, while non-zero eigenvalues correspond to perturbations transverse to the synchronization manifold. For $\gamma_k = 0$, the sign of the largest Lyapunov exponent (LLE) of Eq. (4) determines the dynamical properties of the synchronized nodes: a negative, zero, or positive LLE indicates fixed point, periodic, or chaotic dynamics, respectively. Hence, we consider only non-zero γ_k in order to determine the stability of global synchronization. The MSF is the LLE of Eq. (4) as a function of the complex number z; for a given network topology, global synchronization is stable for values of the coupling strength ϵ for which the MSF is negative for all $z = \epsilon\gamma_k$. We note that while the unperturbed Laplacian matrix of Network 2 is non-diagonalizable (and therefore has only two non-zero eigenvalues), it has been shown that the MSF formalism still determines the stability of global synchronization [27].

Figure 5 shows the zero contour of the MSF for both periodic ($\beta = 1.35$) and chaotic ($\beta = 4.5$) nodes. It turns out that the zero contours (points where the LLE is zero) are circles in the complex plane centered at $z = 1$ whose radii generally decrease with increasing β. This zero contour is critical for determining the stability [19, 20]. When all $\epsilon\gamma_k$ are inside the circle, the LLE is negative and global synchronization is stable. However, when an eigenvalue moves outside as an effect of structural modifications, the LLE of the corresponding mode becomes positive and global synchronization is unstable. Therefore, in this setting, the condition for stability of the considered network with time-delayed coupling is $|1-\epsilon\gamma_k| < r_0$, for all nonzero eigenvalues, where r_0 is the radius of the zero contour of the MSF, which depends on the dynamical properties of the synchronized nodes [19, 20].

Figure 5 also shows all $\epsilon\gamma_k$ of the initial and final networks. As before, we have chosen ϵ such that global synchrony is stable in the initial network. Consequently, the $\epsilon\gamma_k$ of the unperturbed networks are inside the zero contours. However, when improving the network connectivity by adding a link, one or more of the $\epsilon\gamma_k$ move outside the contour, resulting in the destabilization of global synchrony.

IV. UNDIRECTED NETWORKS

Undirected networks are a special case in which the coupling is reciprocal. Because of this additional symmetry, the spectrum and the eigenvectors of the Laplacian are real. Therefore, the motion of the eigenvalues upon the addition of extra links can occur only along the real axis. Hence, in undirected networks, upon the addition of a link we can in principle observe only two paths to instability: *A*) the smallest γ_k can decrease across the left boundary of the zero contour, or *B*) the largest γ_k can increase across the right boundary of the zero contour. While both mechanisms are a result of eigenvalues leaving the stability circle, they correspond to different physical mechanisms of desynchronization. The former corresponds to the intuitive case in which the coupling strength is too small to support synchronization of the modified network; it has recently been shown that this is impossible for undirected networks [11]. The latter case *B*), however, is possible for undirected networks and corresponds to the case in which the coupling is too strong to permit global synchrony in the modified network.

Consider the undirected network of time-delayed oscillators depicted in Fig. 1(c), where the coupling links of the initial network are shown as solid black lines, and the added link is shown as a dotted (red online) line.

Results of simulating Equations (1) and (2) for this network configuration are presented in Fig. 6. As before, the nodes start from random initial conditions. The initial network coupling is turned on at $t = 40$ ms, and synchronous dynamics are observed. At $t = 120$ ms, the new link is added, destabilizing the synchronized state. Our simulations predict the desynchronization of the network upon the addition of the link for both periodic ($\beta = 1.35$) and chaotic ($\beta = 3.0$) node dynamics. Typical uncoupled node dynamics are shown in the inset of Fig. 6. The values of ϵ were chosen such that the initial networks synchronize.

We also test these predictions in a real experimental network of optoelectronic oscillators. We first test the stability of global synchrony on the initial network. Then, starting from different random initial conditions, we test the stability with the new link added. Figure 7 shows experimental measurements for the periodic and chaotic cases on the undirected network. We find that

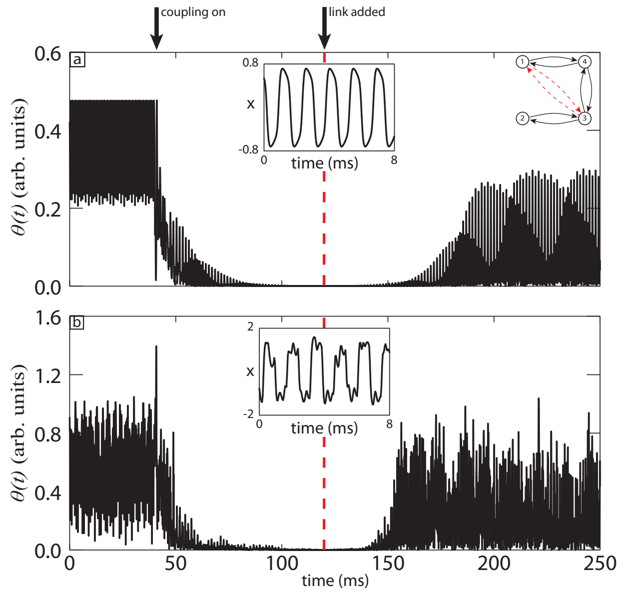

FIG. 6. (color online) Simulated loss of synchrony upon the addition of a link for the undirected network shown. The new link is added at $t = 120$ ms, indicated by the dashed line. The synchronous dynamics are periodic ($\beta = 1.35$) for (a) and chaotic ($\beta = 3.0$) for (b). Inset: Dynamics of a single uncoupled node.

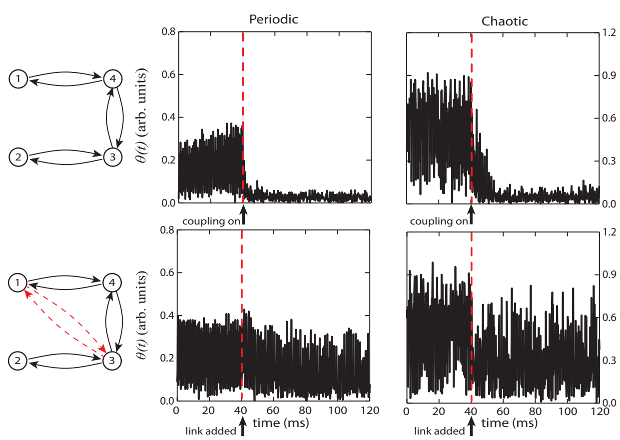

FIG. 7. (color online) Experimental results for the undirected network. The nodes are initially uncoupled. The coupling scheme depicted to the left is implemented at t=40 ms as indicated by the dashed line. For the periodic case, $\epsilon = 0.55$ and for the chaotic case $\epsilon = 0.50$.

the experiment and simulation agree: Global synchronization is stable in the initial network and unstable in the network with the added link.

We now investigate the stability of the network using the MSF, calculated from Eq. (4) and presented in Fig. 8. The addition of the undirected link causes the largest eigenvalue to increase across the right boundary of the zero contour. Thus, the network experiences loss of global synchrony due to the coupling being too strong

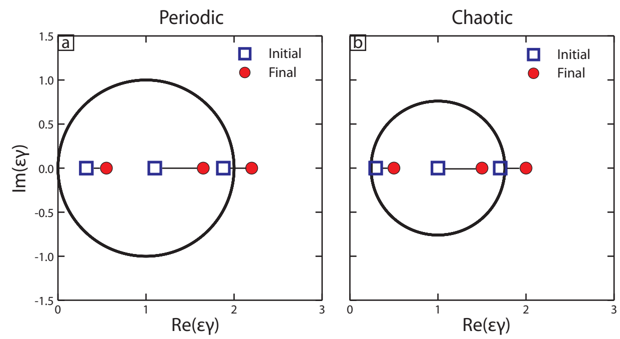

FIG. 8. (color online) MSF and Laplacian eigenvalue spectra for the Undirected Network. (a) Periodic node dynamics ($\beta = 1.35$). (b) Chaotic node dynamics ($\beta = 3.0$). The eigenvalues of the original network are represented by □, and those of the network with the link added are represented by ●. The black line denotes the zero contour of the MSF: Inside global synchrony is stable; outside it is unstable.

to permit synchronization of the modified network.

V. EFFECTS OF DIRECTIONALITY IN LARGE NETWORKS

In the previous examples we considered rather small networks. If the network is large it seems reasonable to assume that the effect of adding a single link is comparably small. This is true for undirected networks. Indeed, for a single eigenvalue λ of the Laplacian $\boldsymbol{L}$, and the corresponding family of eigenvalues $\lambda(\epsilon)$ of the perturbed Laplacians $\boldsymbol{L}_\epsilon = \boldsymbol{L} + \epsilon\boldsymbol{\delta}$ we have that

$$\lambda(\epsilon) = \lambda + \lambda'(0)\epsilon + O(\epsilon^2),$$

with

$$\lambda'(0) = \frac{\langle \boldsymbol{x}, \boldsymbol{\delta y}\rangle}{\langle \boldsymbol{x}, \boldsymbol{y}\rangle}$$

where $\boldsymbol{x}$ and $\boldsymbol{y}$ are normalized left and right eigenvectors of $\boldsymbol{L}$ corresponding to λ and $\langle\cdot,\cdot\rangle$ is the Euclidean inner product, see Ref. [11]. Now for undirected networks we have that $\boldsymbol{y} = \boldsymbol{x}$, and hence $\lambda'(0) \leq \epsilon\|\boldsymbol{\delta}\|$. So, independent of the coupling topology, the slope of the eigenvalue can be bound by the size of the perturbation. In the case of a directed network however, this is not true. More precisely, the case can occur where the left and right eigenvectors $\boldsymbol{x}$ and $\boldsymbol{y}$ are almost orthogonal, leading to a large slope of the eigenvalue.

To illustrate this essential difference between directed and undirected networks consider the example network from Fig. 9. In the undirected network obtained by ignoring the links' directions in Fig. 9(a), the spectral gap is $\lambda_2 = 1.4345$. Increasing the weight on the bold (red) link in Fig. 9(b) in both directions by one yields a slight increase of about 8×10^{-4}. On the other hand, the directed network in Fig. 9(a) has a simple spectral gap

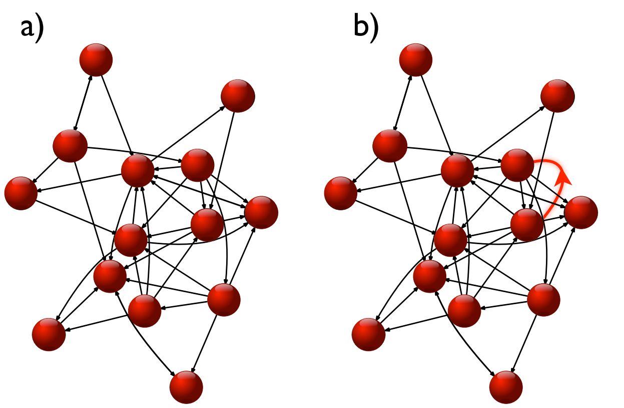

FIG. 9. (color online) A network of 14 nodes. Adding the link as indicated in b) decreases the spectral gap essentially. For the underlying undirected network, increasing the weight on the same link increases the spectral gap by 4 orders less.

$\lambda_2 = 0.8464$ where adding a directed link as indicated in Fig. 9(b) yields a drastic decrease of the spectral gap by 0.5722 (at the same time the maximal eigenvalue increases by $3 \cdot 10^{-3}$). And indeed, the left and right eigenvectors of the Laplacian are almost orthogonal with a degree of 89.7°. For the sake of illustration we have chosen an example with fourteen nodes. However, this same mechanism can be used for much larger directed networks in order to obtain a considerable decrease of the spectral gap just by adding a simple link.

For a global nonlinear estimate on the behavior of the eigenvalues under perturbations, the Bauer-Fike theorem implies that for undirected networks the eigenvalue cannot move much. That is, consider the spectral gap λ_2 of the Laplacian $\boldsymbol{L}$ and let $\tilde{\lambda}_2$ denote the spectral gap of perturbed Laplacian $\tilde{\boldsymbol{L}} = \boldsymbol{L} + \varepsilon\boldsymbol{\delta}$. Next, recall that the Laplacian $\boldsymbol{L}$ can be written in its spectral decomposition $\boldsymbol{L} = \boldsymbol{S}\boldsymbol{\Lambda}\boldsymbol{S}^{-1}$. Then we obtain that $|\lambda_2 - \tilde{\lambda}_2| \leq \kappa(\boldsymbol{S})\|\boldsymbol{\delta}\|$, where $\|\cdot\|$ is the induced Euclidean norm and $\kappa(\boldsymbol{S}) = \|\boldsymbol{S}\|\|\boldsymbol{S}^{-1}\|$ is the condition of the matrix $\boldsymbol{S}$. For undirected networks, we have $\|\boldsymbol{S}\| = \|\boldsymbol{S}^{-1}\| = 1$. So the change of the spectral gap can be bound by the size of the perturbation, independently of the topology of the network. In directed networks however, the topology can play a major role in terms of the eigenvectors of L as the matrix $\boldsymbol{S}$ can get close to noninvertible.

VI. DISCUSSION

For certain classes of coupling functions such as in the Kuramoto model and the power-grid model (more generally, for the classes studied in Refs. [27–29]) the MSF is unbounded. That is, the stability condition is $\epsilon\mathrm{Re}(\gamma_2) > \gamma_c$ for some $\gamma_c > 0$, where γ_2 is the Laplacian spectral gap. Hence, scenario A) is the only one possible for synchronization loss: network modifications must decrease the real part of the smallest eigenvalue in order to destabilize the synchronous state. As noticed in [11], under this stability condition there is a sharp distinction between undirected and directed networks. Because in undirected networks it is not possible to decrease the smallest eigenvalue by adding a link, this destabilization scenario occurs exclusively in directed networks.

In systems with time-delayed coupling, the MSF is bounded in every direction by the stability circle, so the stability of synchronization is determined by the eigenvalue with the largest complex magnitude. This has drastic consequences for both undirected and directed networks. The presence of time delay in the coupling creates an instability that permits undirected networks to destabilize under the addition of a link which increases the largest eigenvalue, as observed in our experiments. The general case of directed networks is significantly more complicated by the time delay because the eigenvalues can be complex. Hence, in addition to scenarios A) and B) mentioned above, the eigenvalues can leave the stability region by changing any combination of the real and imaginary parts of the eigenvalues, as our experiments have demonstrated. A major challenge is to predict which network modification will lead to synchronization loss for an arbitrary network. If we restrict to modifications with small weights, by using perturbation of eigenvalues [11] it is possible to determine all the links that will lead to synchronization loss. For links with large weight, tracking both the motion of eigenvalues and eigenvectors is well known to be a difficult nonlinear problem. In general, the addition of a few links can lead to large changes in the network eigenvalues, even for large networks [28].

The networks considered here all have uniform coupling delays. In some real-world networks, the coupling delays are not equal for all links, which complicates and, in some cases, inhibits synchronization, except for the simplest case of periodic oscillators or fixed-point steady-state solutions. In such cases, the effect of adding or subtracting of links must be considered in the broader context of how network inhomogeneity affects the synchronization [30–34].

In conclusion, we have examined the loss of synchrony upon the addition of a link in both undirected and directed networks of four optoelectronic oscillators with time-delayed couplings. We have found that the presence of time delay in the coupling plays a crucial role in the synchronization behaviors of both types of networks. While our experiment is restricted to network of 4 nodes, our analysis is general and can be applied to networks of arbitrary size. The destabilization scenario is purely dynamical and directly related to the changes in the network spectrum which cause the appearance of unstable modes. We have discussed the synchronization loss mechanisms in terms of the network structure, node dynamics and coupling functions. These results shed light on recent findings where synchronization loss was observed as a consequence of connectivity improvements [5–7, 10, 11]. Furthermore, they offer strategies to design network modifications that guarantee the network's overall synchronization performance.

Acknowledgments: We thank C.R.S. Williams for helpful discussions regarding the experiment. This work was partially supported by DFG/FAPESP grant IRTG 1740/TRP 2011/50151-0 and EU Seventh Framework Programme ERC Grant Agreement 33952. We gratefully acknowledge Grant #: N000141410443 from ONR for supporting the research at the University of Maryland, College Park.

---

[1] F. Sivrikaya and B. Yener, IEEE Network **04** (2004).
[2] E. Bollt, Int. J. Bif. Chaos **22**, 1250261 (2012).
[3] J. Milton and P. Jung, eds., *Epilepsy as a Dynamic Disease* (Springer, 2003).
[4] T. Nishikawa and A. E. Motter, Proc. Nat. Ac. Sci. USA **73**, 065106 (2010).
[5] L. Huang, K. Park, Y.-C. Lai, and K. Yang, Phys. Rev. Lett. **97** (2006).
[6] M. Jalili, IEEE Transactions on Neural Networks and Learning Systems **24**, 1009 (2013).
[7] D. Witthaut and M. Timme, New J. Phys. **14**, 083036 (2012).
[8] D. Witthaut and M. Timme, The European Physical Journal B **86**, 1 (2013).
[9] T. Coletta and P. Jacquod, arXiv preprint arXiv:1505.07998 (2015).
[10] P. Menck, J. Heitzig, J. Kurths, and J. Schellnhuber, Nature Comm. **5**, 1 (2013).
[11] J. P. Pade and T. Pereira, Sci. Rep. **5** (2015).
[12] K. Josić, J. M. López, W. Ott, L. Shiau, and M. R. Bennett, PLoS Comp. Bio. **7**, e1002264 (2011).
[13] A. Goel and D. V. Buonomano, Phil. Trans. R. Soc. B **369**, 20120460 (2014).
[14] J. W. Stahlhut, T. J. Browne, G. T. Heydt, and V. Vittal, IEEE Transactions on Power Systems **23**, 84 (2008).
[15] M. S. Yeung and S. H. Strogatz, Physical Review Letters **82**, 648 (1999).
[16] D. Hunt, G. Korniss, and B. K. Szymanski, Phys. Rev. Lett. **105**, 068701 (2010).
[17] S. Heiligenthal, T. Dahms, S. Yanchuk, T. Jüngling, V. Flunkert, I. Kanter, E. Schöll, and W. Kinzel, Phys. Rev. Lett. **107**, 234102 (2011).
[18] D. J. Jörg, L. G. Morelli, S. Ares, and F. Jülicher, Phys. Rev. Lett. **112**, 174101 (2014).
[19] V. Flunkert, S. Yanchuk, T. Dahms, and E. Schöll, Phys. Rev. Lett. **105**, 254101 (2010).
[20] V. Flunkert, S. Yanchuk, T. Dahms, and E. Schöll, J. Math. Sci. **202**, 809 (2014).
[21] T. E. Murphy, A. B. Cohen, B. Ravoori, K. R. Schmitt, A. V. Setty, F. Sorrentino, C. R. S. Williams, E. Ott, and R. Roy, Phil. Trans. R. Soc. A **368**, 343 (2010).
[22] B. Ravoori, A. B. Cohen, J. Sun, A. E. Motter, T. E. Murphy, and R. Roy, Phys. Rev. Lett. **107**, 034102 (2011).
[23] C. R. S. Williams, T. E. Murphy, R. Roy, F. Sorrentino, T. Dahms, and E. Schöll, Phys. Rev. Lett. **110**, 064104 (2013).
[24] C. R. S. Williams, F. Sorrentino, T. E. Murphy, and R. Roy, Chaos **23**, 043117 (2013).
[25] L. Larger, Phil. Trans. R. Soc. A **371**, 20120464 (2013).
[26] L. M. Pecora and T. L. Carroll, Phys. Rev. Lett. **80**, 2109 (1998).
[27] T. Pereira, J. Eldering, M. Rasmussen, and A. Veneziani, Nonlinearity **27**, 501 (2014).
[28] C. W. Wu, Physics Letters A **319**, 495 (2003).
[29] T. Pereira, D. Eroglu, G. Bagci, U. Tirnakli, and H. Jensen, Phys. Rev. Lett. **110**, 234103 (2013).
[30] F. Sorrentino and M. Porfiri, EPL (Europhysics Letters) **93**, 50002 (2011).
[31] J. Sun, E. M. Bollt, and T. Nishikawa, EPL (Europhysics Letters) **85**, 60011 (2009).
[32] F. M. Atay, Physical review letters **91**, 094101 (2003).
[33] S. Jalan and A. Singh, Physical Review E **90**, 042907 (2014).
[34] C. Masoller and A. C. Marti, Physical review letters **94**, 134102 (2005).